ARTICLE

Imaging Pancreatic Cancer Using Bioconjugated InP Quantum Dots

Ken-Tye Yong,[†,*] Hong Ding,[†] Indrajit Roy,[†] Wing-Cheung Law,[†] Earl J. Bergey,[†] Anirban Maitra,[‡] and Paras N. Prasad[†,*]

[†]Institute for Lasers, Photonics and Biophotonics, University at Buffalo, The State University of New York, Buffalo, New York 14260-4200, and [‡]Department of Pathology and Oncology, The Sol Goldman Pancreatic Cancer Research Center CRB-2, Suite 345, Johns Hopkins University School of Medicine, 1550 Orleans Street, Baltimore, Maryland 21231

ABSTRACT In this paper, we report the successful use of non-cadmium-based quantum dots (QDs) as highly efficient and nontoxic optical probes for imaging live pancreatic cancer cells. Indium phosphide (core)—zinc sulfide (shell), or InP/ZnS, QDs with high quality and bright luminescence were prepared by a hot colloidal synthesis method in nonaqueous media. The surfaces of these QDs were then functionalized with mercaptosuccinic acid to make them highly dispersible in aqueous media. Further bioconjugation with pancreatic cancer specific monoclonal antibodies, such as anticlaudin 4 and antiprostate stem cell antigen (anti-PSCA), to the functionalized InP/ZnS QDs, allowed specific *in vitro* targeting of pancreatic cancer cell lines (both immortalized and low passage ones). The receptor-mediated delivery of the bioconjugates was further confirmed by the observation of poor *in vitro* targeting in nonpancreatic cancer based cell lines which are negative for the claudin-4-receptor. These observations suggest the immense potential of InP/ZnS QDs as non-cadmium-based safe and efficient optical imaging nanoprobes in diagnostic imaging, particularly for early detection of cancer.

KEYWORDS: quantum dots · bioconjugates · bioimaging · pancreatic cancer · targeted delivery

Semiconductor nanocrystals, or so-called quantum dots (QDs), possess unique optical properties that make them potential candidates as luminescent nanoprobes for biological applications, ranging from immunoassays to live cell and tissue imaging.[1−13] Such nanomaterials have significant advantages over traditional fluorescent probes such as organic dyes and fluorescent proteins.[14−17] For example, they have robust photochemical stability, high quantum yield, and excellent resistance to chemical and photochemical degradation, as well as size-tunable photoluminescence that ranges from visible to near-IR with sharp spectral bands.[6,18,19] Also, QDs with different emission colors can be simultaneously excited with a single light source, with minimal spectral overlap, providing significant advantages for multiplexed detection of molecular targets.[20−22] More importantly, QDs can be tuned to emit in a range of wavelengths by systematically changing the nanoparticle size, shape, and composition, whereas new architecture of organic dyes must be designed to shift their emission toward desirable optically detectable wavelengths.[9,21] Thus, these QDs have recently attracted much attention as new generation probes for optical bioimaging.[6,23−28]

One major drawback which severely limits the potential for clinical translation of QDs is the toxicity concern of common use of II−VI semiconductor (such as CdSe and CdTe) QDs in biomedical applications. These semiconductor nanoparticles are easily disintegrated in biological systems if their surfaces are not carefully modified with shell coatings, biocompatible polymers, and biomolecules. Therefore, in recent years, the emphasis has shifted toward the fabrication of non-cadmium-based QDs for applications in biology. In this direction, QDs made up of III−V semiconductors (such as InP) are extremely promising as they are not only cadmium free but also more robust structurally owing to the presence of covalent bonds in their matrix.[29−31] This structural robustness confers enhanced optical stability and, most importantly, reduced toxicity as a result of non-erosion of constituent ions in biological systems.[32] For example, it was reported that Syrian golden hamsters survived throughout a two-year observation period, where they were given 3 mg/kg InP particles intratracheally for 8 weeks.[33] Our group has demonstrated the use of folic acid−InP QD bioconjugates for confocal and two-photon imaging of KB cancer cells.[29,34] Also, our group has recently shown that the optical properties of the core−shell structures were strongly dependent on the nature of the shell around InP. By simply coating the InP core with a ZnS, ZnSe, and CdSe shell, the emission

*Address correspondence to kyong2@buffalo.edu, pnprasad@buffalo.edu.

Received for review May 5, 2008 and accepted February 16, 2009.

Published online February 25, 2009. 10.1021/nn8008933 CCC: $40.75

wavelength can be systematically tuned from ~525 to ~590 and from ~590 to ~680 nm, respectively.[1] These features have made InP QDs a very attractive candidate for replacing cadmium-based QDs for biological studies. However, to date, there are very little studies reporting the use of InP QDs in bioimaging applications, as they are difficult to prepare because of the sensitivity of precursors and surfactants toward the reaction environment in obtaining good quality InP QDs.[29] We have successfully overcome these challenges by using a simple one-pot synthesis approach in fabricating high-quality InP/ZnS QDs.[35]

Pancreatic cancer ranks as the fourth leading cause of cancer related deaths in the United States. The mean survival rate is estimated to be 6 months, and less than 5% of all patients diagnosed with pancreatic cancer survive beyond 5 years.[36,37] This dismal scenario is primarily due to the fact that most patients are diagnosed when the cancer has reached an advanced stage, which is the result of a lack of specific symptoms and limitations in diagnostics that allows the disease to elude detection during its formative stages.[38] Thus, it is critical that novel targeted bioimaging probes be developed which would specifically diagnose pancreatic cancer *in vivo* at their earliest stage, without exerting any systemic toxicity. Nontoxic InP-based QDs with high luminescence and ease of linkage with cancer-specific targeting ligands are therefore ideal candidates for this purpose.[27,39]

We here present the use of InP/ZnS QDs as targeted optical probes for labeling human pancreatic cancer cells, both immortalized and low passage ones. Antibodies such as anticlaudin 4 and anti-PSCA, whose corresponding antigen receptors are known to be overexpressed in both primary and metastatic pancreatic cancer, were utilized for the synthesis of QD bioconjugates.[40−42] The mercaptosuccinic acid functionalized InP/ZnS QDs were conjugated with antibodies using carbodiimide chemistry. To our knowledge, no study has been reported on the use of antibody−InP/ZnS QD bioconjugates as targeted optical probes for live pancreatic cancer cell imaging. With confocal microscopy and localized spectroscopy, we demonstrate receptor-mediated uptake of QD−antibody bioconjugates into pancreatic cancer cells. Also, we have found that the InP/ZnS QDs have very low cytotoxic effect on the cells, thereby justifying our strategy of using them for targeted bioimaging.

RESULTS AND DISCUSSION

Scheme 1 illustrates the surface functionalization and bioconjugation of QDs for cellular targeting and imaging. The first step involves the ligand exchange process of myristic acid capped QDs with mercaptosuccinic acid in the organic phase. The mercaptosuccinic acid coated QDs with carboxyl groups being terminated on their surface are readily dispersible in water. Next, the mercaptosuccinic acid coated QDs are conjugated with targeting biomolecules by using the carbodiimide chemistry.

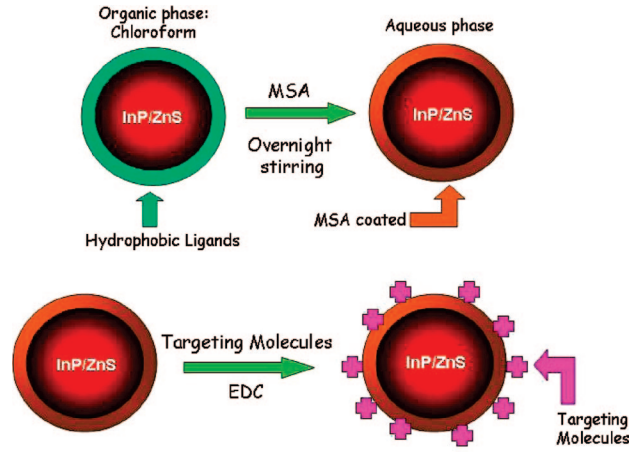

Scheme 1. Schematic illustration showing the formation of the water-dispersible InP/ZnS QD bioconjugates.

The InP/ZnS QDs were systematically characterized by transmission electron microscopy (TEM) and powder X-ray diffraction (XRD). Panels a and b of Figure 1 show the TEM images of InP/ZnS QDs with a diameter of 15−20 nm at low and high resolution, respectively. The powder XRD pattern from the InP/ZnS QDs is shown in Figure 2. All of the diffraction peaks from the four samples can be readily indexed to the zinc blende InP. The three strong peaks with 2θ values of 26.05, 30.15, and 43.15° correspond to the (111), (220), and (311) planes, respectively.

Figure 3a shows the absorption and photoluminescence (PL) spectra of InP/ZnS in chloroform. The QDs demonstrate an absorption feature at ~645 nm and a band edge emission at ~650 nm. The PL quantum yield

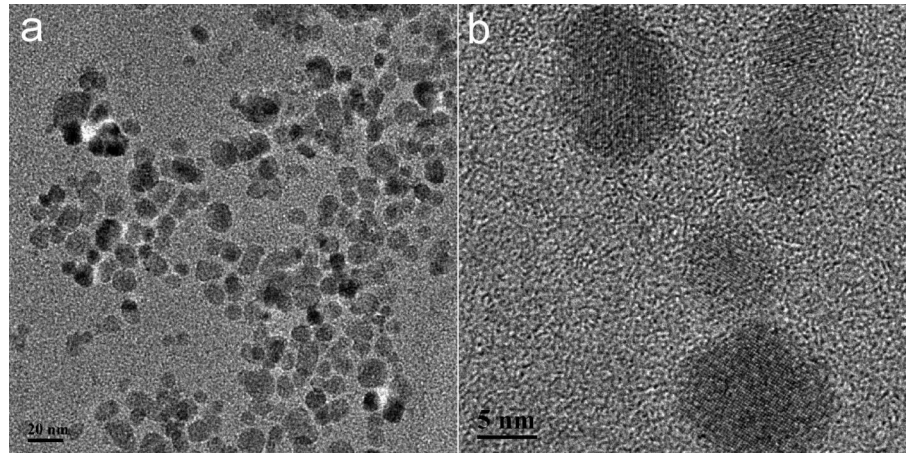

Figure 1. (a,b) TEM image of water-dispersible InP/ZnS QDs at different magnification.

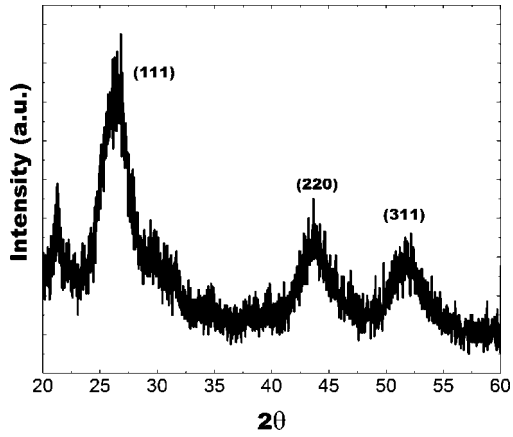

Figure 2. XRD profile of InP/ZnS QDs.

(QY) of the InP/ZnS QDs is estimated to be 25−30%. The QY was measured by comparing the emission of the QD with that of a fluorophore with known QY (rhodamine 6G), at normalized absorption. The QY value, although not as high as that for the cadmium-based quantum dots, is still sufficient for live cell imaging studies. The solution containing mercaptosuccinic acid coated InP/ZnS QDs did not show any significant decrease in the photoluminescence intensity for 2 days, even after conjugating them with an antibody.

The optical stability of the mercaptosuccinic acid coated InP/ZnS QDs under different pH was examined. Figure 3b shows the PL intensity of the InP/ZnS QDs from acidic to basic pH conditions. In changing the pH from 3.3 to 10.8, more than 35% of variation in the PL intensity is observed, although they remain stable for more than 48 h. Even with a ~38% decrease in PL intensity at neutral pH, there is still sufficient photoluminescence intensity for cell imaging studies in our case (see below). At pH 10.8, a ~40% loss of their PL was observed immediately, and further loss of the PL intensity was observed after 1−2 days of storage at room temperature. However, it is worth mentioning that, for the InP/ZnS QDs dispersion in the pH range of 3.3−8.5, the band edge emission of PL spectra was still maintained even after storing them for more than 2−3 days. The mercaptosuccinic-coated InP/ZnS QDs also exhibit stable PL for more than 1 week when dispersed in common physiological buffers such as PBS and MES.

DLS was used to estimate the size distribution of the prepared nanoparticle suspensions. Figure 4a shows the effective size as well as size distributions of InP/ZnS particle suspensions in 1× PBS. From Figure 4a, it is evident that the particles in 1× PBS buffer have an average effective diameter of ~33 nm. According to our TEM results, the size of the InP/ZnS particles is 15−20 nm. This does not directly agree with the DLS data. However, TEM only measures the size of the inorganic semiconductors and does not consider the surface cap-

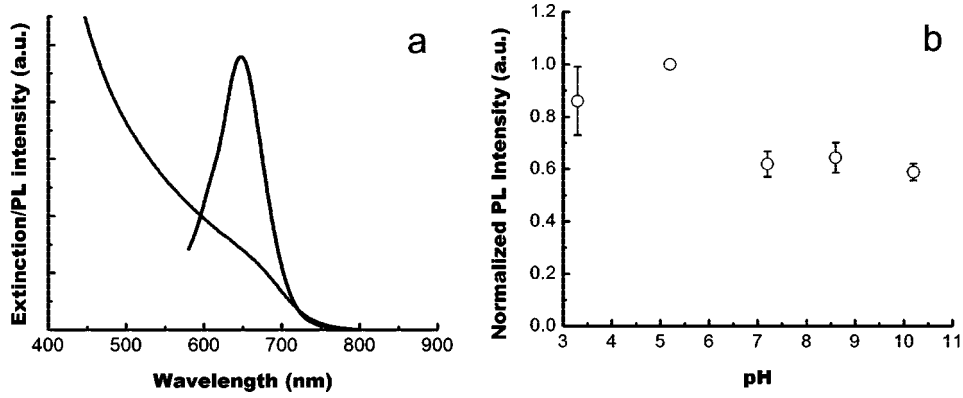

Figure 3. (a) Absorption and emission spectra of InP/ZnS QDs dispersed in chloroform. (b) Photoluminescence stability of InP/ZnS QDs under different pH conditions after dispersing the QDs for 48 h.

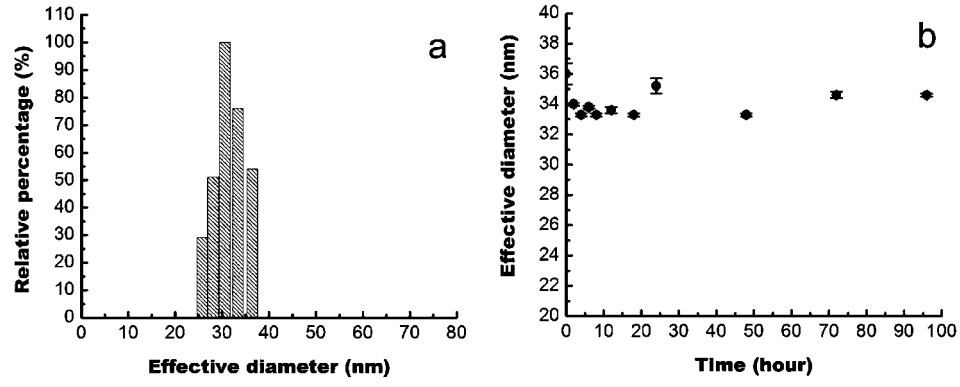

Figure 4. (a) DLS plot of InP/ZnS QDs water dispersion. (b) Time dependence of hydrodynamic diameter of InP/ZnS QDs dispersed in PBS buffer.

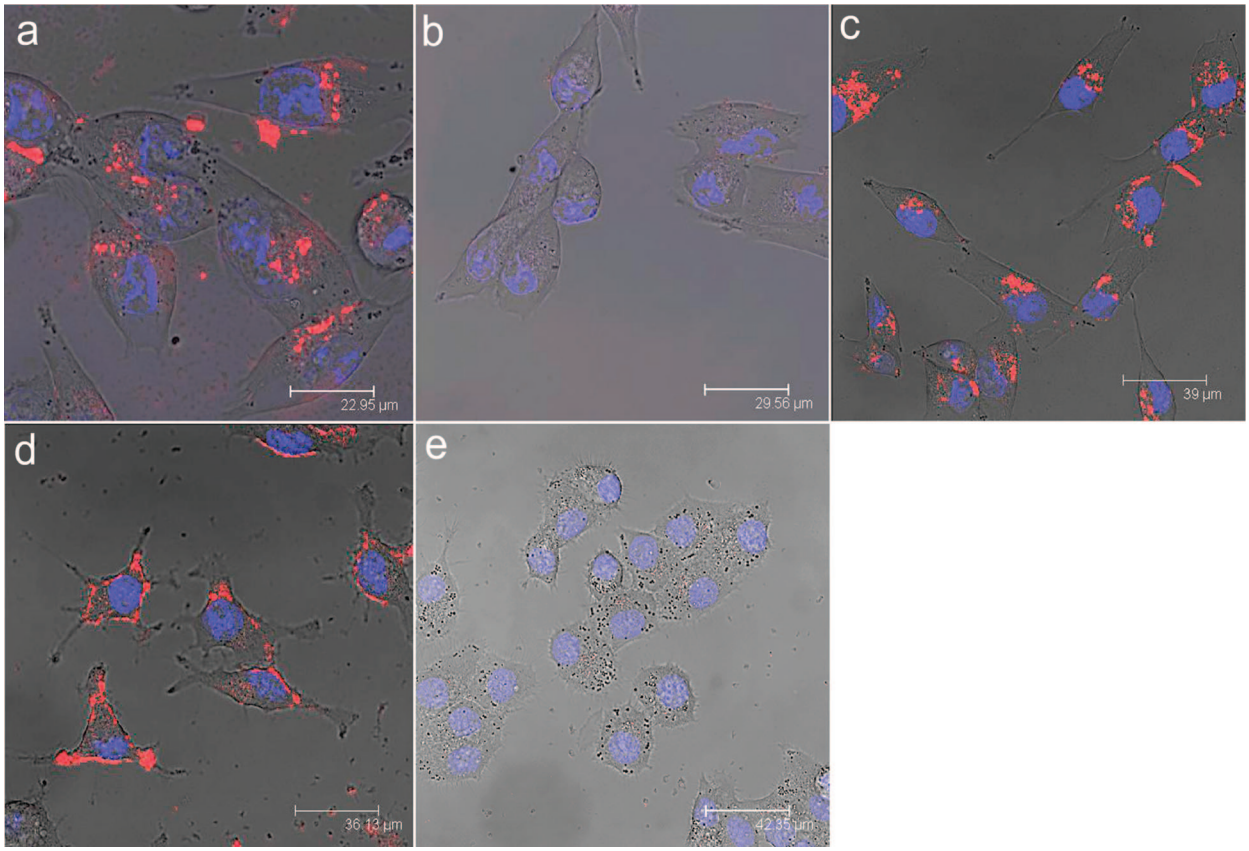

Figure 5. Confocal microscopic images of (a) MiaPaCa cells treated with anticlaudin 4-conjugated InP/ZnS QDs; (b) MiaPaCa cells treated with unconjugated InP/ZnS QDs; (c) MiaPaCa cells treated with anti-PSCA-conjugated InP/ZnS QDs; (d) XPA3 cells treated with anticlaudin 4-conjugated InP/ZnS QDs; and (e) KB (human nasopharyngeal epidermal carcinoma cell line) cells treated with anticlaudin 4-conjugated InP/ZnS QDs. In all cases, blue represents emission from Hoechst 33342 and red represents emission from InP/ZnS QDs.

ping surfactants. The results of the DLS experiments demonstrate the hydrodynamic diameter of the particles that includes the overall size of the solvated capping ligands. A similar trend in size measurements between DLS and TEM has been observed in the previous reports.[29]

In this study, DLS was also used to determine the colloidal stability of the InP particles dispersed in the PBS buffer. Figure 4b shows the time-dependent profile of the effective diameter of the QDs. Over the time range from 0 to 90 h, the effective diameter varies by less than 10%, indicating that their colloidal stability is not affected under physiological pH. In addition, we want to emphasize that the result shown here is to demonstrate the nonaggregation of the QDs under physiological conditions.

One of the greatest challenges in preparing a stable aqueous dispersion of nanoparticles involves the selection of small, biocompatible, and low toxicity hydrophilic ligands to replace the hydrophobic moieties on the surface of the QDs. An appropriate ligand improves the overall colloidal stability of the QDs, which is essential to obtain successful bioconjugation.[20] We have found that the mercaptosuccinic acid coated QDs are more optically and colloidally stable than the "traditional" mercaptoacetic acid coated QDs. This may be due to the presence of two carboxyl groups in the mercaptosuccinic acid molecule. Also, with the mercaptosuccinic acid coated QDs, we were able to maintain the consistency of conjugating biomolecules with the QDs using the carbodiimide chemistry. So far, we have successfully conjugated transferrin, folic acid, monoclonal antibodies, polyclonal antibodies, and other proteins to the QDs. These bioconjugates can be used to label cells without any obvious loss of photoluminescence. We have observed that mercaptoacetic acid coated QDs are found to be more toxic than the mercaptosuccinic acid coated QDs when they are used for labeling cells at high concentration (~10 μg/mL). This finding suggests that the surfactants are also playing a critical role in contributing to the overall toxicity level of the functionalized QDs.

In the *in vitro* study, we used InP/ZnS QDs to label human pancreatic cancer cells (MiaPaCa or Panc-1). The QDs were conjugated with anticlaudin 4, whose corresponding antigen receptors are known to be overexpressed in both primary and metastatic pancreatic cancer.[43] Figure 5a illustrates labeling of pancreatic cancer cells (MiaPaCa) with the bioconjugates, anticlaudin 4−InP/ZnS QDs. Cellular uptake of the QD bioconjugates can be clearly observed from the robust optical signal of the MiaPaCa cells, while no or little signal is ob-

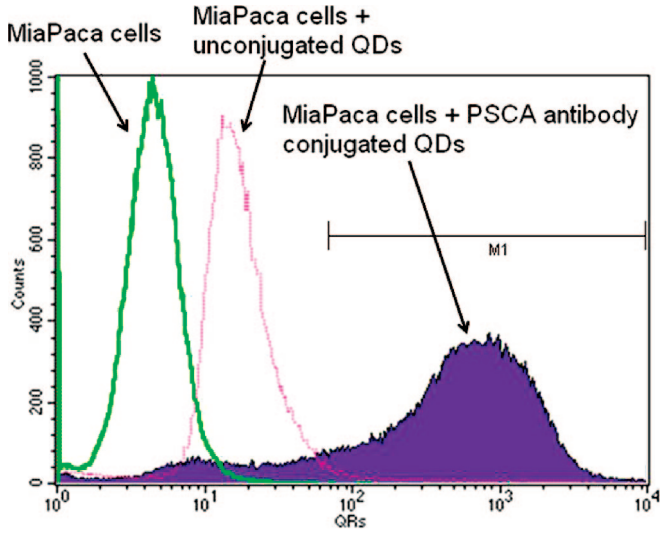

Figure 6. Flow cytometry data showing the relative uptake of unconjugated QDs and PSCA-conjugated QDs in MiaPaCa cells. The number of positively labeled cells was represented as the percentage of total cell counts.

served in the case of cells treated with nonbioconjugated QDs (see Figure 5b), which demonstrates the specific nature of the antibody-mediated targeting of the pancreatic cancer cells. Local spectral analysis of the overall cell staining by the bioconjugated QDs confirms the origin of cellular luminescence signal from the InP/ZnS QDs. More importantly, no signs of morphological damage to the cells were observed upon treatment with various QDs, thereby illustrating their low cytotoxicity. The observed staining pattern is indeed due to the functionalized QDs, which have been demonstrated by several reports.[19,29,44−46] In addition to monoclonal antibody conjugation, QDs were also conjugated with a polyclonal antibody, anti-PSCA, for specific targeting of human pancreatic cancer cells. Figure 5c shows confocal images of MiaPaCa pancreatic cancer cells labeled with anti-PSCA−QD bioconjugates. A strong uptake of the anti-PSCA−QD bioconjugates was also observed. These prepared QD bioconjugates (both monoclonal and polyclonal antibodies) were also further tested in a low passage pancreatic cancer cell line XPA3, and a similar labeling trend was observed (see Figure 5d). From these results, it clearly shows that the engineered InP/ZnS bioconjugates can serve as a potential biocompatible targeted nanoprobe to specifically diagnose human pancreatic cancer cells.

To further confirm a receptor-mediated uptake of the bioconjugates, receptor-negative cells (human nasopharyngeal epidermal carcinoma cell line, also known as KB) for claudin-4 were treated with anticlaudin 4−InP/ZnS bioconjugates. A significantly reduced uptake of both the QD bioconjugates in KB cells was observed (see Figure 5e) compared to that for Panc-1 and MiaPaCa cells under similar conditions. This experiment confirms "active" targeting, or the receptor-mediated nature of labeling of pancreatic cancer cells with the bioconjugated QDs.

In addition to receptor-negative cell lines, flow cytometry was used to quantify their luminescence from the treated cells as shown in Figure 6. The fluorescence intensity of untreated cells was in the range between 10^0 and 10^1, and the cells treated with unconjugated QDs exhibited luminescence intensity in the range between 10^1 and 10^2. Thus, the cells that exhibited luminescent intensity higher than 10^2 were taken as positively labeled with bioconjugates. The superior uptake of the bioconjugated nanoparticles is evident from the fact that there is a noticeable change in the luminescence signal observed between unconjugated QDs and antibody-conjugated QDs labeled Panc-1 cells, indicating that the specific uptake capability of the bioconjugates is maintained well after the conjugation with QDs.

So far, cytotoxicity of cadmium-based QDs has been consistently reported for *in vitro* studies.[15,47,48] The cause of cytotoxicity has been suggested to depend on a number of factors including size, capping agents, concentration of QDs, coating materials, and processing parameters.[9] For example, Derfus *et al.* have shown that uncapped CdSe QDs will slowly decompose in aqueous solution and generate Cd^{2+} ions.[47] The Cd^{2+} ion concentration was directly correlated with the cytotoxic effects. Shiohara *et al.* have reported the cytotoxic effects of CdSe/ZnS QDs with different sizes on three different cell types.[49] To our knowledge, no studies were reported on the cyctotoxicity of InP/ZnS QDs. We have examined the cytotoxicity of InP/ZnS QDs using the cell viability (MTS) assay on Panc-1 cells. Figure 7 shows that the viability of treated cells (for both 24 and 48 h) are in the range of 80−90% relative to that of untreated cells, even at a treatment concentration as high as ~300 μg/mL. This safe dosage is 30 and 15 times higher than that of the cyctotoxicity dosage of CdTe[48] and PbSe[50] QDs, respectively. This result strongly indicates that the InP/ZnS QDs have a relatively low cellular cytotoxicity, thereby justifying our

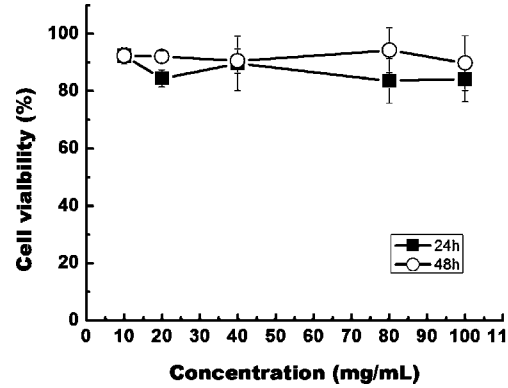

Figure 7. *In vitro* cell viability of MiaPaCa treated with varying concentrations of InP/ZnS QDs for 24 and 48 h. Percentage cell viability of the treated cells is calculated relative to that of untreated cells (with arbitrarily assigned 100% viability).

strategy of using them as non-cadmium-based targeted optical probes for biomedical applications.

To date, many reports have shown the use of cadmium-based QDs for *in vitro* and *in vivo* targeted imaging. However, a major limitation of using cadmium-based QDs is their potential toxicity that is due to the degradation of QDs when their surfaces are not properly functionalized. So far, there are many reports regarding the short- and long-term toxicity caused by cadmium-based QDs.[47,48] In our study, we did not observe any cytotoxicity effects of the InP/ZnS QDs *in vitro* for up to 48 h of treatment. In a recent report, it was reported that no adverse effects were found in mice treated with CdSe QDs. For example, Akerman *et al.* administrated peptide-labeled CdSe/ZnS QDs into mice and studied the tissue distribution.[51] It was found that these functionalized QDs accumulated in the liver and spleen, in addition to the targeted sites, and this nonspecific accumulation was reduced by further modifying the QD surface with PEG molecules. The group reported that no acute toxicity was caused by this QD formulation after 24 h of circulation. Similarly, Larson *et al.* reported that no acute toxicity was observed after injecting CdSe/ZnS QDs into the mice and hypothesized that CdSe/ZnS QDs successfully excrete from the body before the breakdown of surface coating that will cause the leakeage of heavy metals from the core materials.[27] However, it is still debatable whether cadmium-based QDs will eventually degrade in biological environment and cause acute toxicicity in the long-term. Many scientists are currently investigating this issue, but no conclusions on the *in vivo* toxic effects of cadmium-based QDs have been drawn to date. In a recent report from Nie's group, the authors have suggested that if it is revealed in the near future that Cd ions are indeed released during their usage in the biological environment, then, new types of QDs must be developed for advancing the biomedical imaging field.[52] Thus, we suggest that InP/ZnS QDs might be a good alternative probe for replacing cadmium-based QDs for biological use. We have noted that no studies are available in the literature on the toxicity of InP/ZnS particles, and at present, we can only speculate and extrapolate from other relevant *in vivo* studies using indium-based nanoparticles. For *in vivo* studies using InAsP/ZnSe QDs, ~150 pmol of injected QDs contains 22 μg of indium.[53] It was reported that an average American ingests on the order ~10 μg of indium daily from food and water.[53,54] Therefore, despite being composed of potentially toxic materials, the dosage may be small enough that overall toxicity is low. It is worth noting that reports on the development of targeted probes for detecting human pancreatic cancer are very few. Thus, there is an urgency to develop robust imaging agents that can specifically target pancreatic cancer *in vivo*, leading to improved diagnosis at an early stage. We believe that the current work will serve as an important milestone for future *in vivo* studies aimed at an early detection of pancreatic cancer, where the tumor targeting efficiency of multiple pancreatic cancer-specific markers can be simultaneously used.

CONCLUSIONS

In summary, we have synthesized photostable, biocompatible, and water-dispersible InP/ZnS QDs by a facile method. These mercaptosuccinic-coated QDs can be readily conjugated with monoclonal as well as polyclonal antibodies for targeted bioimaging. By using confocal microscopy technique, we have demonstrated the labeling of QD bioconjugates in claudin-4 and PSCA overexpressing pancreatic cancer cells such as MiaPaCa and the low passage cell line, XPA-3. An efficient receptor-mediated uptake of the InP/ZnS bioconjugates in MiaPaCa cells is confirmed by their robust cellular staining, as opposed to the weaker staining of the bioconjugates in receptor-negative (KB) cells. These findings not only offer insights into the receptor-mediated delivery mechanism but also help the design and development of future nanoprobes for *in vivo* cancer detecting and therapeutic applications. InP/ZnS QDs combining the brightness, photostability, and biocompatibility characteristics will serve as a new generation of targeted optical probes for several biomedical applications, including early detection of cancer, replacing the cadmium-based (*e.g.*, CdSe) QDs.

EXPERIMENTAL SECTION

Materials. Indium acetate, sulfur, myristic acid, tristrimethylsilylphosphine, apo-transferrin, octadecene, and HPLC water were purchased from Aldrich. Zinc 2-ethylhexanoate was obtained from Alfa Aesar. All chemicals were used as received. All solvents (hexane, toluene, DMSO, and ethanol) were of reagent grade and used without further purification. Panc-1, MiaPaCa, and KB cells are purchased from ATCC (Manassas, VA). All cell culture media and reagents were obtained from Invitrogen (USA).

One-Pot Synthesis of InP/ZnS Quantum Dots. The synthesis method was adapted from that presented by Lucey *et al.*[35] 4 mmol indium acetate, 6 g of myristic acid, and 5 mL of octadecene were loaded into a 100 mL three-necked flask. Next, the reaction mixture was slowly heated under an argon atmosphere to 180 °C. After 30 min of heating, a clear homogeneous solution was obtained. The reaction mixture was maintained at 180 °C for another 10 min, then 2.6 mL of $P(TMS)_3$ solution (1 g of tristrimethylsilylphosphine $P(TMS)_3$ in 4 mL of octadecene) was rapidly injected. After 10 min of heating, the reaction temperature was lowered to 150 °C. Separately, an oleylamine−sulfur solution was prepared by dissolving 0.1926 g of sulfur (6 mmol) in 5 mL of oleylamine, and zinc 2-ethylhexanoate−octadecene solution was prepared by mixing 2 mL of zinc 2-ethylhexanoate with 5 mL of octadecene. These two mixtures were used for ZnS shell growth. Two milliliters of zinc 2-ethylhexanoate−octadecene solution was injected into the reaction mixture. Then, 2 mL of oleylamine−sulfur solution was added dropwise into the reaction mixture. The reaction mixture was then held at ~210 °C for

45 min, and then an aliquot was removed *via* syringe and was injected into a large volume of toluene at room temperature, thereby quenching any further growth of the QDs. The QDs were separated from the surfactant solution by addition of ethanol and centrifugation. The dark-brown QD precipitate could be readily redispersed in various organic solvents (hexane, toluene, and chloroform).

Preparation of Mercaptosuccinic Acid Functionalized InP/ZnS Quantum Dots. The preparation method of aqueous dispersion of QDs was adapted from that presented by Bharali *et al.*[29] In this reaction, 4 mmol of mercaptosuccinic acid was mixed with 5 mL of chloroform under vigorous stirring. After stirring for 10 to 15 min, 2 mL of concentrated (~10−20 mg/mL) InP/ZnS QDs solution was added into this mixture. Approximately 1 min later, 1 mL of ammonium hydroxide was added to this vigorously stirred solution. This solution was stirred overnight at room temperature. The QDs were separated from the surfactant solution by addition of ethanol followed by centrifugation. The precipitate was redispersed in 5 mL of HPLC water, and the solution was further filtered using a syringe filter with a pore diameter of 0.45 μm. The mercaptosuccinic acid coated QDs have relatively good colloidal stability, and no precipitation was observed after several weeks. This solution was kept in the refrigerator at 4 °C for further use.

Conjugation of Mercaptosuccinic Acid Coated InP/ZnS QDs with Transferrin. The preparation method for an aqueous dispersion of transferrin−QD bioconjugates was adopted from our previous report.[46] From the diluted stock solution, 100 μL of mercaptosuccinic acid coated QD stock solution was mixed with 200 μL of 2.5 mM EDC solution and gently stirred for 1 to 2 min. Next, 200 μL of transferrin was added into this mixture and incubated at room temperature for 2 h to allow the protein to covalently bond to the lysine-coated QDs.

Conjugation of Mercaptosuccinic Acid Coated QDs with Antibodies. The preparation method of aqueous dispersion antibody−QD bioconjugates was adopted from that presented by Yong *et al.*:[19] 100 μL of mercaptosuccinic acid coated QD stock solution was mixed with 100 μL of 2.5 mM EDC solution and 300 μL of water. The mixture was gently stirred for 1 to 2 min. Next, 7 μL of anticlaudin 4 (500 μg/mL) was added into this mixture and incubated at room temperature for 2 h. In this study, we estimated that there are at least 1−2 antibodies per QD.

Cell Staining Studies. For *in vitro* imaging with QDs, the established human cancer cell lines Panc-1, MiaPaCa, and KB were cultured in Dulbecco minimum essential media (DMEM) with 10% fetal bovine serum (FBS), 1% penicillin, and 1% amphotericin B. In addition, low passage pancreatic cancer cells (XPA-3) were also used, cultured in RMPI-1640 medium with 10% fetal bovine serum (FBS), 1% penicillin, and 1% amphotericin B. The day before treatment, an appropriate number of cells was seeded in 35 mm culture dishes. On the treatment day, the cells (at a confluency of 70−80%) in serum-supplemented media were treated with the antibody-conjugated QDs for 2 h at 37 °C (1−5 μg/mL). Nuclei were then stained with Hoechst 33342 (10 μM, 1 h; λ_{em} 461 nm). After 2 h, the cells were washed three times with PBS and directly imaged in a confocal microscope. In order to confirm that the expression of membrane proteins and the binding of targeted QDs to these proteins is not simply an artifact of long-term passage in established cell lines, we also validated the targeting experiments using XPA3, a low passage cell line established at the Johns Hopkins University. These low passage lines retain many of the biological properties observed in the *in vivo* tumor setting by virtue of their limited *ex vivo* passage numbers.[55]

Cellular Imaging. Confocal microscopy images were obtained using a Leica fluorescence imaging system with laser excitation at 405 nm. All images were taken with the exact same conditions of laser power, aperture, gain, offset, and scanning speed.

Characterization Methods. The absorption spectra were collected using an Agilent 8453 UV−visible spectrophotometer over the range from 300 to 1100 nm. The samples were measured against water as reference. All samples were loaded into a quartz cell for measurements. Transmission electron microscopy (TEM) images were obtained using a JEOL model JEM-100CX microscope with an acceleration voltage of 100 kV. The specimens were prepared by drop-coating the sample dispersion onto a carbon coated 300 mesh copper grid, which was placed on a filter paper to absorb the excess solvent. X-ray powder diffraction patterns were recorded using a Siemens D500 diffractometer, with Cu Kα radiation. A concentrated QD dispersion was drop cast onto a quartz plate for measurement. Emission quantum yields (QYs) of the QDs' chloroform dispersion were determined by comparing the integrated emission from the QDs to rhodamine 6 dye solutions of matched absorbance. Samples were diluted so that they were optically thin. The effective size distribution of the QD suspensions was estimated using a dynamic light scattering particle size analyzer (Brookhaven 90Plus fitted with APD detector using a 656 nm laser). The InP/ZnS particles were dispersed in 1× PBS at a concentration of 1 mg/mL for the measurement. These solutions were filtered through a 0.45 μm syringe filter membrane to remove the dust impurities and then analyzed directly.

Cell Viability. For each MTS assay, 24 culture wells (8 sets, each set contains 3 wells) of Panc-1 cell were prepared. Seven sets were treated with different concentration of InP/ZnS QDs, and the remaining one set was the control. The complete assay was performed three times, and results were averaged. Various concentrations of QDs ranging from 25 to 350 μg/mL were added to each well and subsequently incubated with the cells for 24 and 48 h at 37 °C under 5% CO_2. As described in the literature, the absorbance of formazan (produced by the cleavage of MTS by dehydrogenases in living cells) is directly proportional to the number of live cells. After the incubation, 150 μL of MTS reagent was then added to each well and well mixed. The absorbance of the mixtures at 490 nm was measured by using a UV−visible spectrophotometer. The cell viability was calculated as the ratio of the absorbance of the sample well to that of the control well and expressed as a percentage.

Flow Cytometry Analysis. The cellular uptake of QDs, with and without conjugation with various targeting molecules, was quantified by flow cytometry. MiaPaCa cells were seeded at 1.0 × 10^6 cells per T25 flask and allowed to attach for 24 h. To determine the extent of QD uptake, the cells were incubated with 25 μL of nanoparticle (~1 mg/mL) solution per 1 mL serum-free medium for 2 h. Treated cells were then washed three times with phosphate-buffered saline (PBS) and then harvested by trypsinization. The QDs served as the luminescent marker to quantitatively determine their cellular uptake, and the results are analyzed by the FACS Calibur flow cytometry and CellQuest Pro software (Becton Dickenson, Mississauga, CA).

Acknowledgment. This study was supported by grants from the NCI RO1CA119397 and the John R. Oishei Foundation. K.T.Y. is supported by the AACR-Pancreatic Cancer Action Network Fellowship for Pancreatic Cancer Research. K.T.Y. is indebted to the reviewers for their helpful comments.

REFERENCES AND NOTES

1. Prasad, P. N. *Nanophotonics*; Wiley: Hoboken, NJ, 2004.
2. Prasad, P. N. *Introduction to Biophotonics*; Wiley-Interscience: Hoboken, NJ, 2003.
3. Arya, H.; Kaul, Z.; Wadhwa, R.; Taira, K.; Hirano, T.; Kaul, S. C. Quantum Dots in Bio-imaging: Revolution by the Small. *Biochem. Biophys. Res. Commun.* **2005**, *329*, 1173–1177.
4. Azzazy, H. M. E.; Mansour, M. M. H.; Kazmierczak, S. C. From Diagnostics to Therapy: Prospects of Quantum Dots. *Clin. Biochem.* **2007**, *40*, 917–927.
5. Bruchez, M., Jr.; Moronne, M.; Gin, P.; Weiss, S.; Alivisatos, A. P. Semiconductor Nanocrystals as Fluorescent Biological Labels. *Science* **1998**, *281*, 2013–2016.
6. Jamieson, T.; Bakhshi, R.; Petrova, D.; Pocock, R.; Imani, M.; Seifalian, A. M. Biological Applications of Quantum Dots. *Biomaterials* **2007**, *28*, 4717–4732.
7. Liu, W.; Choi, H. S.; Zimmer, J. P.; Tanaka, E.; Frangioni, J. V.; Bawendi, M. Compact Cysteine-Coated CdSe(ZnCdS) Quantum Dots for *In Vivo* Applications. *J. Am. Chem. Soc.* **2007**, *129*, 14530–14531.

8. Liu, W.; Howarth, M.; Greytak, A. B.; Zheng, Y.; Nocera, D. G.; Ting, A. Y.; Bawendi, M. G. Compact Biocompatible Quantum Dots Functionalized for Cellular Imaging. *J. Am. Chem. Soc.* **2008**, *130*, 1274–1284.
9. Wolcott, A.; Gerion, D.; Visconte, M.; Sun, J.; Schwartzberg, A.; Chen, S.; Zhang, J. Z. Silica-Coated CdTe Quantum Dots Functionalized with Thiols for Bioconjugation to IgG Proteins. *J. Phys. Chem. B* **2006**, *110*, 5779–5789.
10. Yong, K. T.; Qian, J.; Roy, I.; Lee, H. H.; Bergey, E. J.; Tramposch, K. M.; He, S.; Swihart, M. T.; Maitra, A.; Prasad, P. N. Quantum Rod Bioconjugates as Targeted Probes for Confocal and Two-Photon Fluorescence Imaging of Cancer Cells. *Nano Lett.* **2007**, *7*, 761–765.
11. Yong, K. T.; Sahoo, Y.; Choudhury, K. R.; Swihart, M. T.; Minter, J. R.; Prasad, P. N. Shape Control of PbSe Nanocrystals Using Noble Metal Seed Particles. *Nano Lett.* **2006**, *6*, 709–714.
12. Yong, K. T.; Sahoo, Y.; Choudhury, K. R.; Swihart, M. T.; Minter, J. R.; Prasad, P. N. Control of the Morphology and Size of PbS Nanowires Using Gold Nanoparticles. *Chem. Mater.* **2006**, *18*, 5965–5972.
13. Yong, K. T.; Sahoo, Y.; Swihart, M. T.; Prasad, P. N. Shape Control of CdS Nanocrystals in One-Pot Synthesis. *J. Phys. Chem. C* **2007**, *111*, 2447–2458.
14. Chan, W. C. W.; Nie, S. Quantum Dot Bioconjugates for Ultrasensitive Nonisotopic Detection. *Science* **1998**, *281*, 2016–2018.
15. Dubertret, B.; Skourides, P.; Norris, D. J.; Noireaux, V.; Brivanlou, A. H.; Libchaber, A. *In Vivo* Imaging of Quantum Dots Encapsulated in Phospholipid Micelles. *Science* **2002**, *298*, 1759–1762.
16. Konkar, A.; Lu, S.; Madhukar, A.; Hughes, S. M.; Alivisatos, A. P. Semiconductor Nanocrystal Quantum Dots on Single Crystal Semiconductor Substrates: High Resolution Transmission Electron Microscopy. *Nano Lett.* **2005**, *5*, 969–973.
17. Yong, K.-T.; Sahoo, Y.; Swihart, M. T.; Prasad, P. N. Growth of CdSe Quantum Rods and Multipods Seeded by Noble Metal Nanoparticles. *Adv. Mater.* **2006**, *18*, 1978–1982.
18. Romero, M. J.; vandeLagemaat, J.; Mora-Sero, I.; Rumbles, G.; Al-Jassim, M. M. Imaging of Resonant Quenching of Surface Plasmons by Quantum Dots. *Nano Lett.* **2006**, *6*, 2833–2837.
19. Yong, K.-T.; Roy, I.; Pudavar, H. E.; Bergey, E. J.; Tramposch, K. M.; Swihart, M. T.; Prasad, P. N. Multiplex Imaging of Pancreatic Cancer Cells by Using Functionalized Quantum Rods. *Adv. Mater.* **2008**, *20*, 1412–1417.
20. Michalet, X.; Pinaud, F. F.; Bentolila, L. A.; Tsay, J. M.; Doose, S.; Li, J. J.; Sundaresan, G.; Wu, A. M.; Gambhir, S. S.; Weiss, S. Quantum Dots for Live Cells, *In Vivo* Imaging, and Diagnostics. *Science* **2005**, *307*, 538–544.
21. Hild, W. A.; Breunig, M.; Goepferich, A. Quantum Dots: Nano-Sized Probes for the Exploration of Cellular and Intracellular Targeting. *Eur. J. Pharm. Biopharm.* **2008**, *68*, 153–168.
22. Xu, G.; Yong, K.-T.; Roy, I.; Mahajan, S. D.; Ding, H.; Schwartz, S. A.; Prasad, P. N. Bioconjugated Quantum Rods as Targeted Probes for Efficient Transmigration Across an *In Vitro* Blood-Brain Barrier. *Bioconjugate Chem.* **2008**, *19*, 1179–1185.
23. Ballou, B.; Lagerholm, B. C.; Ernst, L. A.; Bruchez, M. P.; Waggoner, A. S. Noninvasive Imaging of Quantum Dots in Mice. *Bioconjugate Chem.* **2004**, *15*, 79–86.
24. Cai, W.; Shin, D. W.; Chen, K.; Gheysens, O.; Cao, Q.; Wang, S. X.; Gambhir, S. S.; Chen, X. Peptide-Labeled Near-Infrared Quantum Dots for Imaging Tumor Vasculature in Living Subjects. *Nano Lett.* **2006**, *6*, 669–676.
25. Hezinger, A. F. E.; Temar, J.; Gopferich, A. Polymer Coating of Quantum Dots: A Powerful Tool Toward Diagnostics and Sensorics. *Eur. J. Pharm. Biopharm.* **2008**, *68*, 138–152.
26. Jiang, W.; Papa, E.; Fischer, H.; Mardyani, S.; Chan, W. C. W. Semiconductor Quantum Dots as Contrast Agents for Whole Animal Imaging. *Trends Biotechnol.* **2004**, *22*, 607–609.
27. Larson, D. R.; Zipfel, W. R.; Williams, R. M.; Clark, S. W.; Bruchez, M. P.; Wise, F. W.; Webb, W. W. Water-Soluble Quantum Dots for Multiphoton Fluorescence Imaging in Vivo. *Science* **2003**, *300*, 1434–1436.
28. Erogbogbo, F.; Yong, K.-T.; Roy, I.; Xu, G.; Prasad, P. N.; Swihart, M. T. Biocompatible Luminescent Silicon Quantum Dots for Imaging of Cancer Cells. *ACS Nano* **2008**, *2*, 873–878.
29. Bharali, D. J.; Lucey, D. W.; Jayakumar, H.; Pudavar, H. E.; Prasad, P. N. Folate-Receptor-Mediated Delivery of InP Quantum Dots for Bioimaging Using Confocal and Two-Photon Microscopy. *J. Am. Chem. Soc.* **2005**, *127*, 11364–11371.
30. Wang, S.; Jarrett, B. R.; Kauzlarich, S. M.; Louie, A. Y. Core/Shell Quantum Dots with High Relaxivity and Photoluminescence for Multimodality Imaging. *J. Am. Chem. Soc.* **2007**, *129*, 3848–3856.
31. Ahrenkiel, S. P.; Micic, O. I.; Miedaner, A.; Curtis, C. J.; Nedeljkovic, J. M.; Nozik, A. J. Synthesis and Characterization of Colloidal InP Quantum Rods. *Nano Lett.* **2003**, *3*, 833–837.
32. Xie, R.; Battaglia, D.; Peng, X. Colloidal InP Nanocrystals as Efficient Emitters Covering Blue to Near-Infrared. *J. Am. Chem. Soc.* **2007**, *129*, 15432–15433.
33. Yamazaki, K.; Tanaka, A.; Hirata, M.; Omura, M.; Makita, Y.; Inoue, N.; Sugio, K.; Sigimachi, K. Long Term Pulmonary Toxicity of Indium Arsenide and Indium Phosphide Instilled Intratracheally in Hamsters. *J. Occup. Health* **2000**, *42*, 169–178.
34. Schroeder, J. E.; Shweky, I.; Shmeeda, H.; Banin, U.; Gabizon, A. Folate-Mediated Tumor Cell Uptake of Quantum Dots Entrapped in Lipid Nanoparticles. *J. Controlled Release* **2007**, *124*, 28–34.
35. Lucey, D. W.; MacRae, D. J.; Furis, M.; Sahoo, Y.; Cartwright, A. N.; Prasad, P. N. Monodispersed InP Quantum Dots Prepared by Colloidal Chemistry in a Noncoordinating Solvent. *Chem. Mater.* **2005**, *17*, 3754–3762.
36. Hruban, R. H.; Maitra, A.; Kern, S. E.; Goggins, M. Precursors to Pancreatic Cancer. *Gastroenterology Clinics of North America* **2007**, *36*, 831–849.
37. Swierczynski, S. L.; Maitra, A.; Abraham, S. C.; Iacobuzio-Donahue, C. A.; Ashfaq, R.; Cameron, J. L.; Schulick, R. D.; Yeo, C. J.; Rahman, A.; Hinkle, D. A.; Hruban, R. H.; Argani, P. Analysis of Novel Tumor Markers in Pancreatic and Biliary Carcinomas using Tissue Microarrays. *Hum. Pathol.* **2004**, *35*, 357–366.
38. Montet, X.; Weissleder, R.; Josephson, L. Imaging Pancreatic Cancer with a Peptide-Nanoparticle Conjugate Targeted to Normal Pancreas. *Bioconjugate Chem.* **2006**, *17*, 905–911.
39. Nida, D. L.; Rahman, M. S.; Carlson, K. D.; Richards-Kortum, R.; Follen, M. Fluorescent Nanocrystals for Use in Early Cervical Cancer Detection. *Gynecol. Oncol.* **2005**, *99*, S89–S94.
40. Nichols, L. S.; Ashfaq, R.; Iacobuzio-Donahue, C. A. Claudin 4 Protein Expression in Primary and Metastatic Pancreatic Cancer: Support for Use as a Therapeutic Target. *Am. J. Clin. Pathol.* **2004**, *121*, 226–230.
41. Argani, P.; Rosty, C.; Reiter, R. E.; Wilentz, R. E.; Murugesan, S. R.; Leach, S. D.; Ryu, B.; Skinner, H. G.; Goggins, M.; Jaffee, E. M.; Yeo, C. J.; Cameron, J. L.; Kern, S. E.; Hruban, R. H. Discovery of New Markers of Cancer through Serial Analysis of Gene Expression: Prostate Stem Cell Antigen is Overexpressed in Pancreatic Adenocarcinoma. *Cancer Res.* **2001**, *61*, 4320–4324.
42. Argani, P.; Iacobuzio-Donahue, C.; Ryu, B.; Rosty, C.; Goggins, M.; Wilentz, R. E.; Murugesan, S. R.; Leach, S. D.; Jaffee, E.; Yeo, C. J.; Cameron, J. L.; Kern, S. E.; Hruban, R. H. Mesothelin is Overexpressed in the Vast Majority of Ductal Adenocarcinomas of the Pancreas: Identification of a New Pancreatic Cancer Marker by Serial Analysis of Gene Expression (SAGE). *Clin. Cancer Res.* **2001**, *7*, 3862–3868.
43. Nichols, L. S.; Ashfaq, R.; Iacobuzio-Donahue, C. A. Claudin 4 Protein Expression in Primary and Metastatic Pancreatic

Cancer Support for Use as a Therapeutic Target. *Am. J. Clin. Pathol.* **2004**, *121*, 226–230.
44. Jiang, W.; Mardyani, S.; Fischer, H.; Chan, C. W. Design and Characterization of Lysine Cross-Linked Mercapto-Acid Biocompatible Quantum Dots. *Chem. Mater.* **2006**, *18*, 872–878.
45. Jiang, W.; Singhal, A.; Zheng, J.; Wang, C.; Chan, W. C. W. Optimizing the Synthesis of Red- to Near-IR-Emitting CdS-Capped CdTexSe1-x Alloyed Quantum Dots for Biomedical Imaging. *Chem. Mater.* **2006**, *18*, 4845–4854.
46. Qian, J.; Yong, K. T.; Roy, I.; Ohulchanskyy, T. Y.; Bergey, E. J.; Lee, H. H.; Tramposch, K. M.; He, S.; Maitra, A.; Prasad, P. N. Imaging Pancreatic Cancer Using Surface-Functionalized Quantum Dots. *J. Phys. Chem. B* **2007**, *111*, 6969–6972.
47. Derfus, A. M.; Chan, W. C. W.; Bhatia, S. N. Probing the Cytotoxicity of Semiconductor Quantum Dots. *Nano Lett.* **2004**, *4*, 11–18.
48. Cho, S. J.; Maysinger, D.; Jain, M.; Roder, B.; Hackbarth, S.; Winnik, F. M. Long-Term Exposure to CdTe Quantum Dots Causes Functional Impairments in Live Cells. *Langmuir* **2007**, *23*, 1974–1980.
49. Shiohara, A.; Hoshino, A.; Hanaki, K.-i.; Suzuki, K.; Yamamoto, K. On the Cyto-toxicity Caused by Quantum Dots. *Microbiol. Immunol.* **2004**, *48*, 669–675.
50. Tan, T. T.; Selvan, S. T.; Zhao, L.; Gao, S.; Ying, J. Y. Size Control, Shape Evolution, and Silica Coating of Near-Infrared-Emitting PbSe Quantum Dots. *Chem. Mater.* **2007**, *19*, 3112–3117.
51. Akerman, M. E.; Chan, W. C. W.; Laakkonen, P.; Bhatia, S. N.; Ruoslahti, E. Nanocrystal Targeting *In Vivo*. *Proc. Natl. Acad. Sci.* **2002**, *99*, 12617–12621.
52. Smith, A. M.; Duan, H.; Mohs, A. M.; Nie, S. Bioconjugated Quantum Dots for *In Vivo* Molecular and Cellular Imaging. *Adv. Drug Delivery Rev.* **2008**, *60*, 1226–1240.
53. Kim, S. W.; Zimmer, J. P.; Ohnishi, S.; Tracy, J. B.; Frangioni, J. V.; Bawendi, M. G. Engineering InAs/InP/ZnSe III−V Alloyed Core/Shell Quantum Dots for the Near-Infrared. *J. Am. Chem. Soc.* **2005**, *127*, 10526–10532.
54. Zimmer, J. P.; Kim, S. W.; Ohnishi, S.; Tanaka, E.; Frangioni, J. V.; Bawendi, M. G. Size Series of Small Indium Arsenide-Zinc Selenide Core-Shell Nanocrystals and Their Application to *In Vivo* Imaging. *J. Am. Chem. Soc.* **2006**, *128*, 2526–2527.
55. Calhoun, E. S.; Hucl, T.; Gallmeier, E.; West, K. M.; Arking, D. E.; Maitra, A.; Iacobuzio-Donahue, C. A.; Chakravarti, A.; Hruban, R. H.; Kern, S. E. Identifying Allelic Loss and Homozygous Deletions in Pancreatic Cancer without Matched Normals Using High-Density Single-Nucleotide Polymorphism Arrays. *Cancer Res.* **2006**, *66*, 7920–7928.